



# **Role of Multi-detector CT in Imaging of Different Tracheal Lesions**

**Thesis**

**Submitted for partial fulfillment  
Of the M.sc. degree in radiodiagnosis  
By**

**Marwan Mohamed Mohamed El-Toukhy  
MB.,B.Ch.  
Cairo University**

**Supervised by  
Dr.Youssriah Yahia Sabri  
Professor of Radiodiagnosis  
Faculty of Medicine  
Cairo University**

**Dr.Marian Fayek  
Lecturer of Radiodiagnosis  
Faculty of Medicine  
Cairo University**

**Dr. Heba Hany Assal  
Lecturer of Chest Diseases  
Faculty of Medicine  
Cairo University**

**Faculty of Medicine  
Cairo University  
2013**

# ACKNOWLEDGEMENTS

First and above all,  
All thanks to **Allah, The Merciful, The Compassionate.**  
This work would not be a reality without His help.

My deep respects and thanks are owed to,  
**Dr. Youssriah Yahia Sabry**  
Professor of Radiodiagnosis  
Faculty of Medicine, Cairo University  
for her sincere advices, kind guidance and supervision of this  
work.

Words stand short to express my respects and thanks to  
**Dr. Marian Fayek,**  
Lecturer of Radiodiagnosis  
and **Dr. Heba Hany,**  
Lecturer of Chest Diseases,  
Faculty of Medicine, Cairo University  
For their kindness and cooperation in all steps of this work.

I am also delighted to express my deepest gratitude and cordial  
thanks to **my family, my father Prof. Mohamed El-Toukhy,**  
**my mother and last but not least my wife and my son.**  
Without their continuous encouragement and support, I could  
not have finished this work.

***Marwan Mohamed El-Toukhy***

# Abstract

Virtual bronchoscopy is an ideal technique for noninvasive evaluation of the tracheobronchial tree which has the advantage of being a noninvasive procedure that can visualize areas inaccessible to the flexible bronchoscope. It is considered a noninvasive modality for identifying tracheo-bronchial obstructions and endoluminal lesions, as well as for assessing the tracheobronchial tree beyond stenoses.

Multidetector CT has greatly overcome the several limitations associated with routine axial CT images suffice for evaluating many airway abnormalities such as limited ability to detect subtle airway stenoses; underestimation of the cranio-caudal extent of disease; difficulty displaying complex 3D relationships of the airways; and inadequate representation of the airways that are oriented obliquely to the axial plane.

## Key word

dimensional (3D) reconstruction- Multi-detector *CT*-Virtual bronchoscopy

# List of Contents

<i>List of Tables</i> .....	II
<i>List of Figures</i> .....	III
<i>Review of Literatures</i>	
<i>Introduction</i> .....	1
<i>Aim of the Work</i> .....	3
<i>Anatomy of the Trachea</i> .....	4
• Gross anatomy / Histology.....	4
• Innervation and blood supply.....	7
• Lymphatic drainage.....	8
• Surrounding anatomic structures.....	9
<i>Clinical presentations and Modalities of assessment of Tracheal Lesions</i> .....	11
• Clinical presentations.....	11
• Modalities of assessment.....	11
• Non-radiological (Bronchoscopy).....	11
• Radiological .....	12
• Plain radiographs.....	12
• Multi-detector CT scanning.....	13
<i>Pathology and CT Picture of Different Tracheal Lesions</i> .....	17
• Classification of tracheal lesions.....	17
• Lesions associated with narrowing of the trachea.....	18
• Tracheomalacia.....	18
• Tracheal tumors.....	20
• Congenital stenosis.....	24
• Saber sheath trachea.....	25
• Granulomatous diseases of the trachea.....	26
• Tracheoesophageal fistula.....	32
• Relapsing polychondritis.....	34
• Tracheopathia osteochondroplastica.....	35
• Tracheal bronchus.....	38
• Vascular rings and slings.....	39
• Lesions associated with widening of the trachea.....	40
• Tracheal diverticulum (Tracheocele).....	40
• Tracheobronchomegaly (Mounier-Kuhn syndrome).....	41

• Secondary Tracheomegaly.....	43
• Trauma.....	43
• Non-pathologic tracheal calcification.....	45
<i>Patients and methods</i> .....	46
<i>Results</i> .....	50
<i>Case presentation</i> .....	52
<i>Discussion</i> .....	70
<i>Summary and conclusion</i> .....	76
<i>References</i> .....	78
<i>Arabic Summary</i>	

## List of Tables

<i>Table (1):</i> Showing patients' presentation.....	46
<i>Table (2):</i> Virtual bronchoscopy technique done in cardiothoracic imaging unit, Radiology department, Cairo University (Kasr Al Aini).....	48
<i>Table (3):</i> HRCT technique used in (Kasr Al –Aini).....	49
<i>Table (4):</i> Showing different MSCT findings of the trachea.....	50
<i>Table (5):</i> Summarizes the MSCT findings in the cases showing tracheal narrowing... .....	51
<i>Table (6):</i> Summarizes the MSCT findings in the cases with tracheal masses.....	51
<i>Table (7):</i> Presents cases with tracheal calcification.....	51

# List of Figures

<b><u>Figure (1).</u></b> a) Anterior view of the trachea showing its cartilaginous constituents. b) Cross-sectional view showing linings of the trachea.....	6
<b><u>Figure (2).</u></b> Tracheal blood supply. Left anterior view. Note the basically segmental nature of distribution.....	8
<b><u>Figure (3).</u></b> Relationships of trachea to surrounding structures. Note the tight packing of major mediastinal vessels adjacent to the trachea.....	10
<b><u>Figure (4)</u></b> Cartilagenous tracheal rings extend about two-thirds of the circumference (endoscopic view).....	12
<b><u>Figure (5)</u></b> Postero-anterior plain X-ray of the neck showing a large intraluminal lesion on the right side of the trachea.....	13
<b><u>Figure (6)</u></b> Anteroposterior view of 3D CT reconstruction of the trachea showing two focal tracheal stenoses (arrows) .....	14
<b><u>Figure (7)</u></b> A 59-yr-old patient with left-sided malignant mesothelioma and a trachea diverticulum as an incidental finding. Virtual bronchoscopy shows a small opening on the dorsal side of the trachea (a, b), the VB entering the opening (c, d), retroflexing the virtual bronchoscope in the diverticle (e, f) and re-entering of the VB into the trachea (g). 3D reformatting (h) shows a small air-containing lesion protruding from the tracheal wall, the trachea diverticulum.....	16
<b><u>Figure (8).</u></b> CT images in a patient with acquired tracheomalacia. Note the posterior bowing of the membranous portion during inspiration (Right) and the marked collapse of the trachea with bowing of the posterior membranous portion anteriorly during expiration (Left).....	20
<b><u>Figure (9)</u></b> Contrast material-enhanced CT scan obtained at the level of the tracheal carina in a 68-year-old woman with tracheal SCC shows a well-defined nodule in the distal trachea (arrow).....	21

<b><u>Figure (10)</u></b> Adenoid cystic carcinoma in 60-year-old man. Unenhanced transaxial CT scan (3-mm collimation) at level of distal trachea that was obtained using mediastinal window settings shows lobulated and broad-based intraluminal soft-tissue tumor ( <i>arrow</i> ) in anterolateral aspect of distal trachea. Also note marked wall thickening ( <i>arrowheads</i> ).....	22
<b><u>Figure (11)</u></b> .(a) Axial CT slice demonstrates a tracheal papilloma attached to the tracheal wall. (b) The virtual bronchoscopy depicts the irregular walls due to scars and small sessile papillomas attached to the tracheal wall.....	23
<b><u>Figure.(12)</u></b> .Congenital tracheal stenosis in a 3-year-old girl with trisomy 21. (a) Series of axial CT slices demonstrating stenosis in the central third of the trachea. (b) This is more sensitively demonstrated on coronal MPR, which correlates well with the bronchographic appearances (c) ( <i>arrows</i> ). (d) VB also demonstrates mild stenosis of the supracarinal portion of the trachea ( <i>arrowheads</i> ).....	24
<b><u>Figure (13)</u></b> . 64-year-old man with long history of smoking and chronic cough. Contrast-enhanced CT image shows increased anteroposterior-to-lateral dimensions of trachea ( <i>thick arrow</i> ) from smoking-related chronic obstructive pulmonary disease. This finding is characteristic of saber-sheath trachea. Left upper lobe bronchogenic carcinoma ( <i>thin arrow</i> ) is present.....	25
<b><u>Figure (14)</u></b> Trachea, Deposition of amyloid in the lamina propria and hyperplasia of the tracheal epithelium. Scattered lymphocytes and plasma cells are present in the lamina propria. HE. ×400.....	26
<b><u>Figure (15)</u></b> Amyloidosis in a 62-year-old woman with mild chronic shortness of breath. Midsagittal reformatted CT image shows a diffusely calcified tracheal wall.....	27
<b><u>Figure (16)</u></b> CT scan demonstrates an extensive thickening of the walls of the trachea in a patient with tuberculosis.....	28
<b><u>Figure (17)</u></b> High magnification of tracheal lymph node with sarcoid granuloma comprised of epithelioid cells, well defined giant cells and lymphocytes. (Hematoxylin-eosin; 10x10) .....	29

**Figure (18)** 61-year-old man with shortness of breath and history of sarcoidosis. Contrast-enhanced CT images of chest show partially calcified, irregular, nodular thickening of trachea (arrows). Tracheal lumen is narrow and abnormal in shape.....30

**Figure (19).** Transverse scan over the upper part of the trachea (*left*) and coronal oblique reformat along the long axis of the trachea (*right*). Note short concentric stenosis of the subglottic area of the trachea (large arrow). Circumferential thickening of the tracheal wall at the level of the stenosis is visible. Note the presence of two small ulcerations within the posterior wall of the trachea (*small arrows*).....31

**Figure (20)** Photograph of the gross pathologic specimen obtained in a patient with known Wegener granulomatosis shows involvement of the proximal trachea (*T*) and subglottic larynx (*SL*) with necrosis and deformation (arrows).....31

**Figure (21).** Diagram of the main types of EA with or without a (TEF). Type a is EA without a TEF and is often called pure EA. Shown are the blind upper and lower esophageal pouches next to the ringed windpipe (trachea) and the branches (bronchi) which lead to each lung. Type b has a connection (fistula) between the upper pouch and the trachea (a TEF). Type c is by far the most common form of EA and has a fistula between the lower esophagus and the trachea (one form of TEF) with a blind upper pouch. A rare form (1%) is type d with two TEFs, one between both the upper and lower esophageal segments and the trachea. Type e has only a TEF and no EA. This is usually referred to as an H or N shaped fistula and may be 2-4% of this group.....33

**Figure (22):** CT scan of upper thorax showing an acquired tracheoesophageal fistula.....33

**Figure (23).** Inflammatory destruction of cartilage in relapsing polychondritis.....34

**Figure (24)** CT scan, soft tissue window, taken at the level of the distal trachea reveals thickening of the tracheal wall and narrowing of the tracheal lumen (indicated by an arrow), in a patient with relapsing polychondritis.....35

**Figure (25)** Bronchoscopic inspection of the trachea reveals osseous submucosal nodules projecting into the tracheobronchial lumen in a patient with tracheopathia osteochondroplastica.....36



**Figure (26).** 47-year-old woman with chronic cough. Unenhanced CT images show nodular, partially calcified, irregular thickening of trachea (arrows) with posterior sparing; these findings are consistent with tracheopathia osteochondroplastica.....37

**Figure (27)** Axial CT image through the upper thorax demonstrate an anomalous right upper lobe bronchus (arrow) arising directly from the trachea .....38

**Figure (28)** Coronal reformatted CT image shows a double aortic arch, in which the right-sided arch is approximately about the same size as the left.....40

**Figure (29)** Tracheal diverticulum. A, Nonenhanced CT scan of the upper thorax demonstrates a small tracheal diverticulum arising from the right posterior lateral wall of the trachea (arrow). Pleural thickening is also noted in this patient after bilateral lung transplantation for cystic fibrosis. B, Eight-month follow-up CT demonstrates a well-formed, slightly larger tracheal diverticulum (short arrow). C, Mediastinal and lung windows from a contrast-enhanced CT scan through the lung apices in a different patient also demonstrate a diverticulum projecting off the right posterior lateral tracheal wall (arrow).....41

**Figure (30).** Bronchoscopic view of trachea in the patient with Mounier-Kuhn syndrome.....42

**Figure (31).** 70-year-old man with history of melanoma. Sagittal reformatted CT image shows tracheal corrugation (arrows). Overall, findings are consistent with Mounier-Kuhn syndrome.....42

**Figure (32)** CT scan obtained at level of bifurcation of trachea in 31-year-old woman with history of blunt force trauma, shows defect in membranous trachea with air tracking into mediastinum (*arrowhead*). Mediastinal emphysema (*arrows*) can also be seen.....44

**Figure (33)** Cartilage of the trachea and primary bronchi are abnormally calcified, which allows us to see them on these two coronal CT images. Abnormal calcification of the trachea (arrow) is responsible for tracheal wall detail seen on these images. Bifurcation of the trachea at the carina (arrow) into the left and right main bronchi (arrows) is easily seen.....45

## INTRODUCTION

The advent of multi-detector CT has revolutionized imaging of the airways and other thoracic structures. In comparison to single-detector helical CT scanners, multidetector scanners not only provide faster speed, greater coverage, and improved spatial resolution, but also have the unique ability to create images of thick and thin collimation from the same data set (*Hu H et al., 2000, Choi RJ et al., 2001*).

One of the greatest benefits of this new technology is the improved quality of two-dimensional (2D) multi-planar and three-dimensional (3D) reconstruction images. These images break away from the confines of the traditional axial imaging plane and have the potential to facilitate the assessment of a variety of airway disorders.

With regard to the assessment of airway stenoses, multi-planar volume reformation methods aid in the detection of mild stenoses, improve the accuracy of determining the length of stenoses, and aid in the identification of horizontal webs. Review of multi-planar volume-reformatted images has been shown to aid in the planning of stent placement or surgery

Airway imaging is routinely performed at end-inspiration during a single breath-hold. State-of-the-art helical scanners allow the entire central airways to be imaged in less than 5 sec. The speed of the examination is particularly important when imaging patients with airway disorders because many of these patients cannot tolerate the significantly longer breath-hold time required by single-detector CT scanners. Short scanning time is also an advantage for imaging during dynamic breathing or at end expiration in patients with suspected tracheomalacia a condition characterized by excessive collapse of the airway during expiration.

Tracheal stricture caused by damage from cuffed endotracheal tube, tracheostomy or trauma to the neck. Cuff pressure in these devices may exceed the capillary pressure leading to ischemic necrosis and subsequent fibrosis. Assessment of such localized tracheal abnormality can be achieved with contiguous 1.5-5.0 mm collimation scans obtained through the area during a single breath hold.

Relapsing polychondritis is a systemic disease in which the tracheal cartilage is affected by recurrent episodes of inflammation. On CT images, fixed narrowing of the tracheal lumen with associated thickening of the wall is noted.

Amyloidosis is a condition in which a fibrillar protein is deposited in the trachea. Tracheal involvement takes the form of diffuse or multifocal submucosal infiltrates. On CT scan, narrowing of the lumen, wall thickening and calcification is noted.

Tracheomalacia is a clinical disorder associated with softening of the cartilage and loss of structural integrity of the trachea. Both primary and secondary etiologies are recognized. In pediatric patients, prematurity or prolonged mechanical ventilation is often implicated. In adults, many cases are posttraumatic or post-inflammatory with or without complicating infections (*Gaissert HA & Burns J., 2010, Carden KA et al., 2005*).

Tracheopathia osteochondroplastica is a rare idiopathic and usually asymptomatic disorder of older men; this disorder is characterized by multiple osteo-cartilaginous masses adjacent to the tracheal rings of the inner anterolateral wall of the trachea. Radiologically, focal tracheal thickening, calcification of the tracheal rings, multiple calcified tracheal nodules, and long-segment tracheal narrowing are typically seen

Saber-sheath trachea deformity is a pathognomonic finding in patients with chronic obstructive pulmonary disease. The saber-sheath appearance is found when mechanical forces of hyperinflated lungs cause the coronal diameter of the intra-thoracic trachea to narrow and the sagittal diameter to elongate so that the sagittal-to-coronal diameter ratio exceeds 2:1. The extra-thoracic trachea remains normal in configuration. CT may also reveal mild intra-thoracic tracheal wall thickening, frequently with ossification of the tracheal rings.

### **AIM OF THE WORK**

Distinguishing the features of different tracheal lesions using multi-detector CT.

## **ANATOMY OF THE TRACHEA**

### **Gross Anatomy / Histology**

The trachea is a flexible cylindrical tube composed of cartilaginous rings, connected by a fibromuscular membrane and lined internally by mucosa. The trachea facilitates the passage of air between the larynx and the lungs. It is positioned midline in the neck and courses slightly to the right in the upper thorax. It extends from the cricoids cartilage superiorly (at about the level of the sixth cervical vertebra) to the carina inferiorly [*Figure (1a)*]. In deep inspiration the carina may descend to the level of the sixth thoracic vertebra. However, the location of the lower end of the trachea varies with body posture, and with inspiration and expiration. The length of the trachea ranges from 10 to 13 cm, averaging approximately 11 cm (*Pierre S et al ., 2003*).

The skeleton of the trachea is composed of 16 to 20 incomplete hyaline cartilaginous rings that are bound in a tight elastic connective tissue oriented longitudinally. These cartilage rings may calcify with age and two or more cartilages may unite, either partially or fully. Rarely, they may bifurcate posteriorly. The cartilage forms about two thirds of the circumference of the trachea. Because the posterior border of the trachea is formed by fibromuscular membrane, the cross-sectional shape of the trachea is that of the letter D, with the flat side posterior (*Hansell DM et al ., 2010*) .

The first and last cartilaginous rings differ from the rest of the tracheal rings. The first ring, located approximately 1.5 to 2 cm below the true vocal cords, is partly recessed into the broader ring of the cricoid cartilage and is the broadest of all the cartilage rings. The first ring is sometimes merged to the cricoid cartilage or to the second tracheal ring. The second, third, and fourth rings are surrounded anteriorly and laterally by the thyroid gland. The last tracheal ring is thicker and broad, and on its lower border there is a triangular process that curves downward and backward between the origins of the bronchi. The mucosal portions of the posterior trachea are separated from the esophagus by a thin layer of connective tissue. This region is often

referred to as the common party wall, as it separates the trachea in front from the esophagus behind (***Wallace T., 2006***).

The cartilaginous rings allow the tracheal lumen to retain its patency, even in the extreme circumstances of coughing and forced expiration. The diameter of the tracheal lumen, like its length, depends on the height, age, and gender of the individual. In men, tracheal diameter ranges from 13 to 25 mm in the coronal plane and 13 to 27 mm in the sagittal plane. Tracheal diameter is slightly less in women, ranging from 10 to 21 mm in the coronal plane and 10 to 23 mm in the sagittal plane. The tracheal caliber is uniform along its length, and any change in such caliber should raise the possibility of a pathologic condition (***Pierre S et al ., 2003***).

Cross-sectional area correlates most closely with height in children. With increasing age, the transverse section of the tracheal lumen successively assumes the following shapes: round, lunate, flattened, and roughly elliptical. Respiratory cycle, certain maneuvers, and body position also contribute significantly to the variation in lumen shape. During rapid deep inspiration, the thoracic portion of the trachea widens and the cervical portion narrows. The opposite pattern occurs during expiration; the extra-thoracic tracheal lumen increases in size during coughing, valsalva maneuver, or forced expirations, whereas the intra-thoracic portion decreases (***Phillip M. Boiselle et al., 2008***).

The trachea is lined by pseudostratified columnar epithelium that sits on an elastic lamina propria [*Figure (1b)*]. Goblet mucous cells and small subepithelial glands that secrete onto the luminal surface are interspersed among the ciliated columnar cells. There has been recent interest in studying the small intercellular bridges (tight junctions) situated between the ciliated cells. These junctions may explain the observation that cilia in the respiratory tract move in a synchronous and coordinated manner. The cilia beat about 1000 times per minute, propelling the mucous lining upward toward the pharynx, from which it can be coughed up several times a day. Normally, the amount of bronchotracheal secretions expelled is quite small, averaging 10 cc over a 24 hour period (***Hansell DM et al ., 2010***).

Mechanical irritation by endotracheal tubes or suction devices, however, can increase this volume 10-fold. During disease states, the amount and quality of the periciliary fluid and mucous can change, interfering with the drainage and protective functions of the mucosa. Each tracheal cartilage has a perichondrium, continuous with a dense fibrous membrane that is between adjacent cartilages and within the posterior membranous wall (*Pierre S et al ., 2003*) .

The perichondrium and membrane are composed primarily of collagen with some elastin fibers. Smooth muscle fibers (trachealis muscle) are in the membrane posteriorly. Most of these muscle fibers are transverse, attaching to the free ends of the tracheal cartilages and providing alteration in the tracheal cross-sectional area. There are also longitudinal fibers. The trachealis muscle can diminish the caliber of the tracheal lumen or prevent overdistention of the trachea when there is abdominal straining prior to coughing (*Phillip M. Boiselle et al., 2008*).

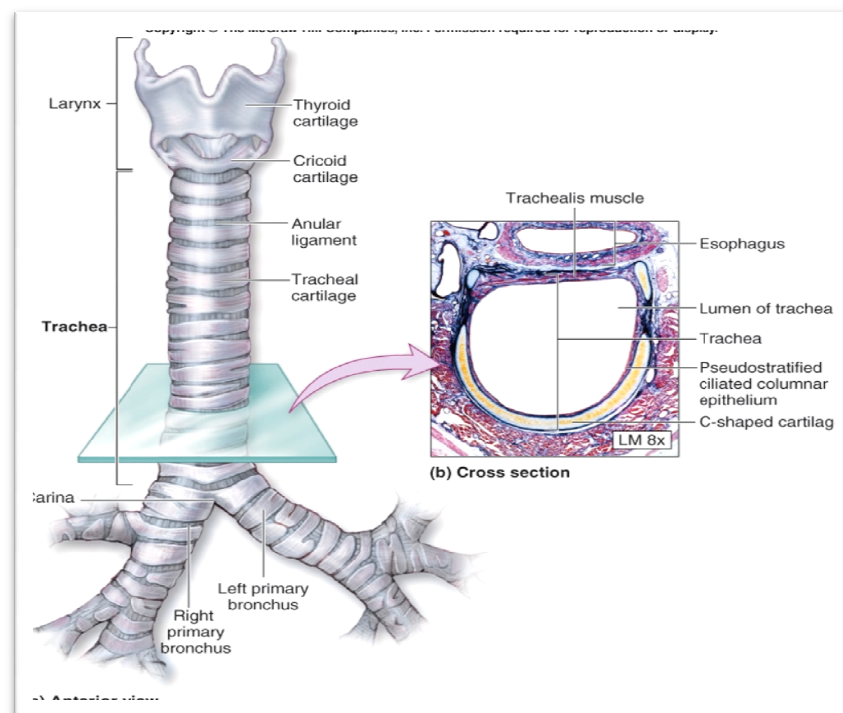


**Figure (1).** a) Anterior view of the trachea showing its cartilaginous constituents. b) Cross sectional view showing linings of the trachea (*Pierre S et al ., 2003*)